Available online at www.sciencedirect.com
ScienceDirect
Catalysis Today 120 (2007) 196–202
CATALYSIS TODAY
www.elsevier.com/locate/cattod

Probing multiple effects of TiO_2 sintering temperature on photocatalytic activity in water by use of a series of organic pollutant molecules

Rosario Enríquez [a,b], Alexander G. Agrios [a,1], Pierre Pichat [a,*]

[a] *Laboratoire "Photocatalyse et Environnement", CNRS, Ecole Centrale de Lyon (STMS), 69134 Ecully Cedex, France*
[b] *Laboratorios de Ingeniería Ambiental, Universidad del Mar, Puerto Ángel, Oaxaca, Mexico*

Available online 8 September 2006

Abstract

Our goal was to determine whether changes induced in TiO_2 by sintering have a net effect on the photocatalytic removal rate of trace organics in water that depends on the organic. To that end, we have used (i) commercialized TiO_2 samples prepared by varying the sintering temperature of the parent TiO_2; (ii) several probe molecules: phenol, anisole, 4-chlorophenol, 2,5-dichlorophenol, 4-chlorobenzoic acid, pyridine and dichloroacetic acid. For aromatics, except pyridine, the removal rates increased with sintering temperature, whereas the opposite was true for pyridine (with one exception) and dichloroacetic acid. These results can be interpreted on the basis of the following hypotheses: decarboxylation requires direct pollutant–TiO_2 contact; pyridine can react by formation of a N-centered radical cation; photocatalytic hydroxylation can occur within the near-surface solution layers. This last hypothesis was checked by comparing the removal rates of some of the probes over powdered TiO_2 to rates over TiO_2 coatings where the accessibility to the TiO_2 surface was restricted by a SiO_2 binder. In practice, the consequences are that one test pollutant does not suffice to quantitatively compare photocatalytic activities, and the selection of an optimal TiO_2 sintering temperature for photocatalytic water treatment depends on the target pollutant(s).

Keywords: TiO_2; Sintering temperature; Benzene derivatives; Dichloroacetic acid; Photocatalysis

1. Introduction

In gas-phase thermal catalysis, an increase in surface area generally improves the catalytic activity. For photocatalytic reactions over semiconductors, the situation is more complex. Increasing the surface area means increasing the density of surface irregularities, such as kinks and edges that introduce additional energy levels in the semiconductor band gap. That effect causes an increase in the recombination rate, k_r, of photo produced charges and hence a decrease in photocatalytic activity. Thus, for instance, sintering a semiconductor can have two opposing effects on the photocatalytic activity by decreasing both k_r and the surface area. This results in the existence of an optimal sintering temperature.

In this study devoted to photocatalytic reactions in the aqueous phase over TiO_2, which remains the most important photocatalyst [1,2], we address the question: Do the changes involved in sintering affect the photocatalytic activity equally whatever the organic reactant? In other words, is the optimum in sintering temperature reactant-dependent? The reason to undertake this investigation is that both the interaction of the trace organic reactant with TiO_2 dispersed in water and the basic photocatalytic mechanism can vary. Accordingly, the effects of k_r and surface area can depend on the organic reactant. Our investigation explores these effects using appropriately chosen TiO_2 samples and organic probe molecules.

Our experiments were conducted using a series of TiO_2 samples manufactured by the same company (Millennium Chemicals) using the same process, differing only in their final sintering temperatures. Consequently, this series is perfectly suited to the present study, as only the parameter of interest, namely the sintering temperature, is varied. Previous studies in our laboratory have examined the photocatalytic behavior of this TiO_2 series for gas-phase and aqueous systems [3–5]. Time-resolved microwave conductivity measurements [6]

* Corresponding author. Tel.: +33 4 78 660550; fax: +33 4 78 331140.
E-mail address: pichat@ec-lyon.fr (P. Pichat).
[1] Present address: Department of Chemistry, Royal Institute of Technology (KTH), Stockholm, Sweden.

0920-5861/$ – see front matter © 2006 Elsevier B.V. All rights reserved.
doi:10.1016/j.cattod.2006.07.054

performed for some of the TiO_2 samples employed here have shown that k_r does decrease when the sintering temperature is increased [7].

We selected a suite of organic probe molecules that would represent a diversity of photocatalytic reaction mechanisms and thereby report from several angles the effects of changing photocatalyst properties. This suite principally included a series of molecules representing simple modifications of benzene: phenol, anisole, 4-chlorophenol (4-CP), 2,5-dichlorophenol (2,5-DCP), 4-chlorobenzoic acid (4-CBA) and pyridine. These molecules exhibit high structural similarity but with a range of electron densities on the aromatic ring, which can be expected to affect reactivity with photocatalytically generated oxidizing species. Phenol and chlorophenols experience abstraction of the hydroxylic H atom and adsorb poorly to TiO_2. Their similarities should allow one to observe to what extent like molecules have similar interactions with the different TiO_2 samples. Dichloroacetic acid (DCAA) was added to the aromatics because it has a carboxylic group in common with 4-CBA and should react predominantly via decarboxylation, since the only C–H bond is not easily broken because of the two neighboring Cl atoms. Also, owing to its carboxylic group, 4-CBA adsorbs better than the other aromatics studied here.

2. Experimental

2.1. Powder TiO_2

Five different types of TiO_2 were used. Four were manufactured by Millennium Chemicals using thermohydrolysis of $TiOSO_4$. The company unfortunately does not reveal the sintering temperatures, except to say that PC105, PC50 and PC10 are made by sintering PC500 at successively higher temperatures. The fifth TiO_2 sample, called Rhodia, was originally synthesized at the laboratory scale as a precursor to Millennium Chemicals' PC series, and is therefore well suited for comparison with the PC samples. It was sintered at a somewhat lower temperature than PC105 as can be inferred from its surface area and mean pore diameter: see Table 1 which shows TiO_2 characteristics provided by Millennium, along with our own previously measured surface areas [4].

2.2. Supported TiO_2

TiO_2 was affixed on thin fiberglass tissues by means of a "size press" [8] using a mixture containing powder TiO_2 and an aqueous colloidal suspension of SiO_2 (particle size: 2–4 nm or 20–30 nm; TiO_2/SiO_2 mass ratio: 1; total mass supported: 80 g/m^2 tissue). The impregnated tissue was allowed to dry at room temperature. The coatings were analyzed by scanning electron microscopy (SEM)–energy-dispersive X-ray microanalysis (EDX) using a Philips XL 20 apparatus and 1 cm^2 samples covered by an Au layer.

Table 1
Physical characteristics of TiO_2 samples

Name	BET surface area ($m^2\ g^{-1}$)	Mean pore diameter (nm)	Particle size (nm)
PC 10	10	24.1	65–75
PC 50	54	20.1	20–30
PC 105	85–95	15.3	15–25
PC 500	317	6.1	5–10
Rhodia	150	8.6	n.d

n.d.: not determined.

2.3. Chemicals

All organics were obtained from Aldrich at 99% or better purity and used without further purification. All water was produced by a Milli-Q Plus system.

2.4. Reactor and light source for photocatalytic degradations

Photocatalytic reactions were performed in a custom cylindrical cell of *ca.* 80 mL volume. The contents were irradiated through the optical bottom window, made of Pyrex and having an area of *ca.* 11 cm^2, with the reactor open to air. A disc of TiO_2-coated tissue could be placed on a glass ring positioned 1 cm above the bottom of the reactor. The light source was a Phillips HPK-125 W high-pressure mercury lamp, with the radiation passing through a 2.2-cm thick circulating water cuvette and a 340 nm cut-off filter before entering the reactor. The irradiation power was *ca.* 33.3 mW cm^{-2} for DCAA, 4-CBA, 2,5-DCP, and 4-CP, and *ca.* 39.5 mW cm^{-2} for phenol, anisole, and pyridine, corresponding to a photon flux of *ca.* 1.75×10^{-7} and 2.08×10^{-7} einstein s^{-1}, respectively.

2.5. Procedures for photocatalytic degradations

The reactor was loaded with 20 mL of an aqueous solution of 4-CBA, 4-CP, 2,5-DCP, DCAA, phenol, anisole or pyridine at the desired concentration and 44 mg TiO_2. This is the same mass of TiO_2 as the amount immobilized on the tissue discs. The slurry was mixed in darkness for at least 1 h before irradiation. Initial concentrations of the pollutants, and some of their properties, are shown in Table 2. Samples were taken for analysis of the initial solution and at various time intervals during reaction.

Table 2
Physical properties and initial concentration of the pollutants studied

Pollutant	Molar weight (g/mol)	Solubility (mg/L)	pK_a	Initial concentration	
				ppm	$\mu mol\ L^{-1}$
4-CBA	156.57	72	3.98	22.8	145.6
4-CP	128.56	2.4×10^4	9.41	21.3	155.1
2,5-DCP	163.00	614	7.51	20.6	126.4
DCAA	128.94	1×10^6	1.26	50.0	165.7
Phenol	94.11	9.8×10^4	9.95	14.5	154.2
Anisole	108.14	1.5×10^3	n.a	16.4	151.8
Pyridine	79.10	Miscible	5.17	11.3	143.4

n.a.: not applicable.

2.6. Sampling

4-CBA, 4-CP, 2,5-DCP and DCAA samples for HPLC analysis were filtered using 0.45-μm Millipore filters into 2-mL amber vials. Phenol, anisole and pyridine samples were prepared for GC analysis with an internal standard, as follows. Sample (400 μL) was drawn into a plastic 1-mL syringe (Codan) and filtered through Millex-HV filters (0.45 μm pores, 4 mm diameter) into a 2-mL amber vial. One hundred microliters of 100 ppmv butan-1-ol was added by glass syringe as the internal standard. The precise amounts of sample and internal standard were determined gravimetrically.

2.7. Analyses

4-CBA, 4-CP and 2,5-DCP were analyzed by HPLC using an LDC Constametric 3200 isocratic pump and an LDC Spectromonitor UV detector set at 240, 226, or 228 nm, respectively. An ODS-2 Waters column (25 cm × 4.6 mm) was used with a mobile phase of methanol/water (60/40 vol.% for 4-CBA; 40/60 vol.% for 4-CP; 55/35 vol.% for 2,5-DCP) flowing at 1 mL/min. For 4-CBA and 4-CP, the pH of the eluent was adjusted to *ca*. pH 3 with H_3PO_4. DCAA was analyzed using a Waters 600 pump and Waters 486 UV detector operated at 210 nm. The mobile phase was 5 mmol L^{-1} H_2SO_4 in water flowing at 0.2 mL/min through an Aminex HPX column.

Phenol, anisole and pyridine were analyzed by GC-FID with a Chrompack CP sil 5CB column (30 m × 0.53 mm × 5 μm) with N_2 as the carrier gas and an H_2/air detector flame. The temperature was 343 K for 2 min followed by a ramp of 10 K/min to 413 K. Five injections of standards were used to determine the relative response factors.

2.8. Apparatus and procedure for oxygen isotopic exchange

The $^{18}O_2$–$Ti^{16}O_2$ isotopic exchange was measured using a sample cell with a 12 cm^2 optical window. A 5.5 cm^2 disk of TiO_2-coated fiberglass tissue was placed in the cell, perpendicular to the irradiation beam. Alternatively, the same mass of TiO_2 was spread as uniformly as possible onto a sample-holder of the same area. The irradiation system was the same as for the aqueous degradation studies. Under UV irradiation, the sample was evacuated, then exposed to 13.3 kPa $^{16}O_2$ (Alphagaz N48) overnight. After evacuation to 10^{-4} Pa, $^{18}O_2$ (98.2 at.% ^{18}O; Yeda R&D Co. Ltd., Israel) was admitted into the cell at the desired pressure in the dark. After equilibration, the sample was UV-irradiated. A variable leak valve allowed periodic analysis of the cell atmosphere by mass spectrometry (Leybold Transpector).

3. Results

3.1. Kinetics of the photocatalytic degradations

The activity of the different TiO_2 samples was characterized by the pseudo-first-order rate constant *k*. The inset in Fig. 1, presented as an example, demonstrates that it was possible to compare photocatalytic removal based on pseudo-first-order kinetics. Taking into account that the sintering temperature of Rhodia is close to that of PC105, Table 3 shows that *k* decreased with increasing sintering temperature for DCAA, whereas it increased for phenol, chlorinated phenols and 4-CBA. The lowest overall proportional increase in *k* was for the aromatic carboxylic acid 4-CBA. For anisole, the order of removal rates over the various TiO_2 samples was generally the same as for the phenols except that, for anisole, the activity of PC105 was slightly higher than that of PC50. The removal rate of pyridine followed the same trend as that of DCAA for PC500, PC105 and PC50; however, PC10 gave the fastest removal.

3.2. Assessment of the accessibility of coated TiO_2

We assessed the surface accessibility of TiO_2 by SEM–EDX, taking advantage of the fact that the penetration depth of the

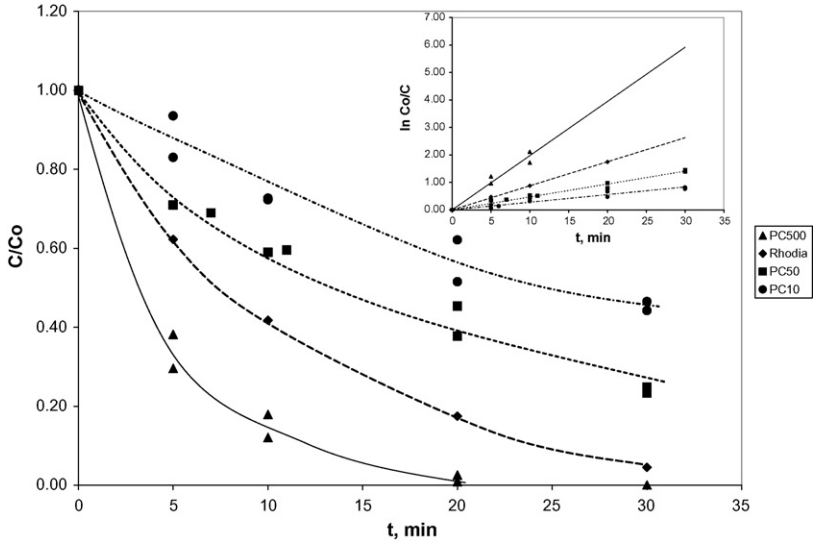

Fig. 1. Photocatalytic degradation of DCAA over the TiO_2 samples indicated. The points plotted correspond to different experiments, not to different analyses. (Inset) Fitting of pseudo-first-order kinetic constant, *k*.

Table 3
Initial pseudo-first-order rate constants k (min^{-1})

TiO_2	DCAA[a]	4-CBA[a]	2,5-DCP[a]	4-CP[a]	Phenol[b]	Anisole[b]	Pyridine[b]
PC500	0.2	0.034	0.013	0.014	0.012	0.004	0.010
PC105	n.d[c]	n.d.	n.d.	n.d.	0.012	0.014	0.007
PC50	0.046	0.06	0.044	0.028	0.024	0.010	0.002
PC10	0.031	0.08	0.05	0.045	0.078	0.132	0.019
Rhodia	0.087	0.05	0.014	0.011	n.d.	n.d.	n.d.

n.d.: not determined.
[a] Radiant power: 33.3 mW cm^{-2}.
[b] Radiant power: 39.5 mW cm^{-2}.

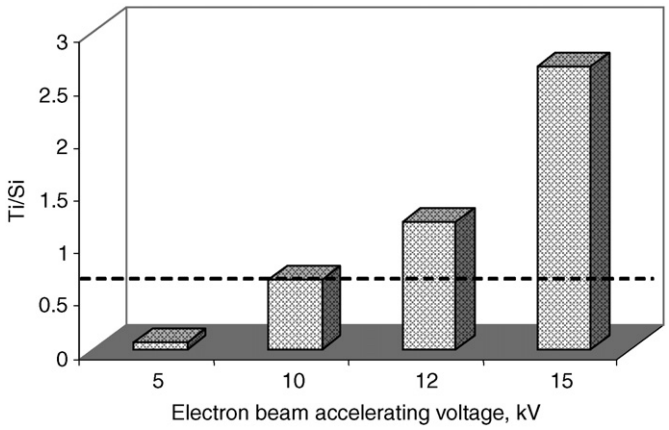

Fig. 2. Variations in the Ti/Si ratio (nominal value: 0.75) vs. the electron accelerating voltage for TiO_2 PC50 and 20–30 nm SiO_2.

electrons, and therefore the coating thickness analyzed, increases with the accelerating voltage. For example, Fig. 2 shows the Ti/Si atomic ratio at different voltages. The overall 1:1 TiO_2/SiO_2 mass ratio corresponds to an atomic ratio of 0.75, yet the figure shows that the SiO_2 resides primarily around the exterior of the coating particles.

The accessibility of TiO_2 to organic solutes cannot be directly determined from the semi-quantitative SEM–EDX results. We have therefore studied the UV-induced $^{18}O_2$–$Ti^{16}O_2$ isotopic exchange, which can only occur with surface oxygen. Fig. 3 shows that, for equal TiO_2 masses and various initial pressures of $^{18}O_2$, the initial isotopic exchange rate (measured as the increase in [$^{18}O^{16}O$] in the headspace) under UV

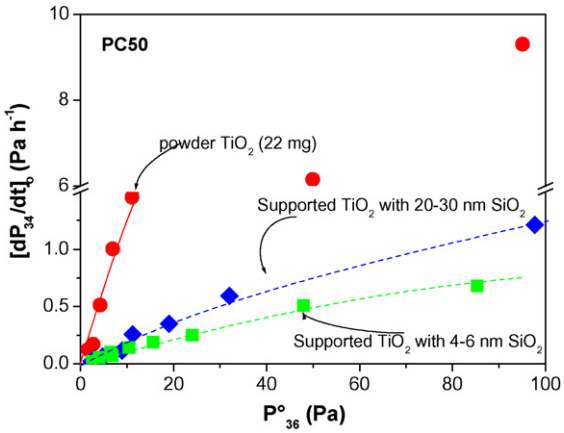

Fig. 3. Photo-induced initial variations in the $^{18}O^{16}O$ pressure vs. the $^{18}O_2$ pressure (at initial equilibrium in the dark) for PC50 TiO_2 and the SiO_2 indicated.

irradiation was sharply reduced when TiO_2 was supported by use of a SiO_2 binder. The smaller the SiO_2 particle size, the slower the isotopic exchange. Clearly, the accessibility of TiO_2 surface oxygen was greatly restricted by the silica binder, which is consistent with the SEM–EDX findings.

3.3. Removal rates of the pollutants over powdered or coated TiO_2

We compared photocatalytic removal rates using the initial rate, r_0, rather than the kinetic rate constant, since the observed kinetics were not always of the same order for affixed TiO_2 (*vide infra*). Reaction rates were reduced on SiO_2-supported particles versus pure, powder TiO_2 to a degree that depended on the probe molecule, the type of SiO_2, the type of TiO_2, and the TiO_2/SiO_2 ratio. We report here only results obtained for a 1:1 mass ratio.

The rate ratios are shown in Fig. 4. The negative effect of SiO_2 on r_0 was especially acute in the case of DCAA removal, where 20–30 nm SiO_2 reduced r_0 to only 1–3% of the value over PC50 or Rhodia powder respectively (Fig. 4, right), and 4–6 nm SiO_2 virtually halted photocatalytic activity (Fig. 4, left).

Coating TiO_2 with SiO_2 also had a pronounced effect on r_0 for 4-CBA removal. Again, the SiO_2 particle size was

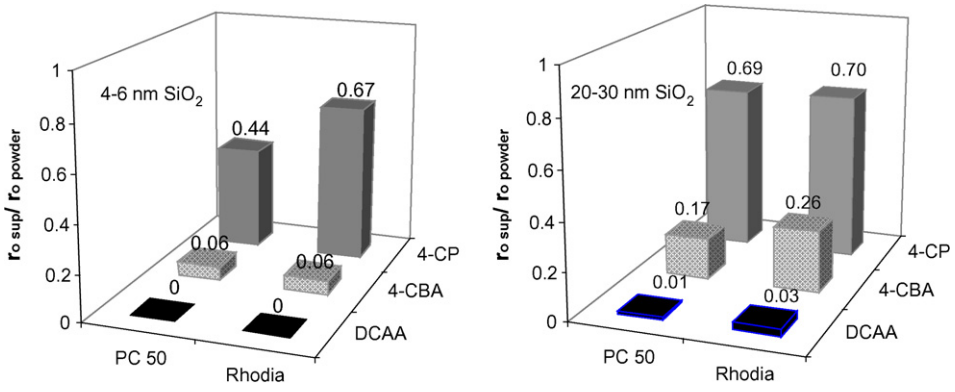

Fig. 4. Ratios of the initial removal rates for supported to powdered TiO_2 for the pollutants and binders indicated.

important; the downward effect on r_0 of 4–6 nm SiO_2 was stronger than that of 20–30 nm SiO_2 by a factor of 2.7–4.3. In addition, the small silica particles lowered the kinetic order of the removal rate to 0, compared to 1 for the larger-particle silica and pure, powder TiO_2 cases. The zero order suggests that the availability of 4-CBA to the surface was not rate-limiting; this implies a greatly restricted area of TiO_2 accessible to the pollutant. This was supported by dark adsorption measurements, which showed significant adsorption of 4-CBA on suspended TiO_2 but none (within detection limits) on supported TiO_2.

To estimate the fraction of supported TiO_2 participating in 4-CBA removal, we analyzed the removal rates of 20 mL of 4-CBA solution over varying amounts of suspended PC50 powder. The activity equalled that of TiO_2 fixed with 20–30 nm SiO_2 when the amount of powdered PC50 was about 2 mg. Thus, in the supported PC50 tissue, only about 4% of the TiO_2 was active in 4-CBA removal.

Fixing the TiO_2 had far less effect on r_0 for 4-CP removal. Furthermore, the effects of the two SiO_2 particle sizes differed by only a factor of about 1.6 for PC50, and were approximately equal for Rhodia. Together, these observations show clearly that restricted access to TiO_2 is less important for 4-CP removal than for 4-CBA or, especially, DCAA removal.

4. Discussion

Clearly, the variations in k (Table 3) for each probe molecule over the various TiO_2 samples were not related to the adsorbed amounts, since the probes for which no adsorption has been detected [3,4] exhibited either an increase in k (phenol, chlorinated phenols and anisole) or a decrease in k (pyridine, with the exception of PC10; *vide infra*) with increasing sintering temperature. Also, for DCAA and 4-CBA, which were significantly adsorbed under the conditions used [4] (undoubtedly because of the carboxylic moiety), opposite variations in k as a function of the sintering temperature were observed.

As mentioned in the introduction, interpreting the net effect of TiO_2 sintering temperature relies on differences of photocatalytic mechanisms depending on the chemical structure of the probe molecules. We hypothesize that hole-mediated attack would require close contact of the molecule with the surface; in contrast, $^{\bullet}OH$ radical-mediated attack could occur not only on the surface, but also within the near-surface solution layers [9–11].

When reported for the first time [12], photocatalytic decarboxylation was proposed to occur by hole-mediated attack. This mechanism should be particularly true for DCAA since, as mentioned in the introduction, the lability of the H atom is very low because of the inductive effect of two Cl atoms on the same C atom. Consequently, the surface area is expected to be a very important factor for the photocatalytic removal rate of DCAA, in agreement with the present observations (Tables 1,3).

It has been shown by comparing photocatalytic and photo-Fenton degradations of benzo[*b*]pyridine (quinoline) that this compound can be attacked by both $^{\bullet}OH$ radicals (predominantly on the benzene moiety) and holes (predominantly on the pyridine moiety) [13]. By use of superoxide dismutase [13] and monohalogenated quinolines [14], the latter mechanism was suggested to involve reaction between superoxide and the N-centered radical cation resulting from hole transfer. Accordingly, it is understandable that as the sintering temperature is increased, the net removal rate of pyridine will decrease, as the reduced recombination rate k_r is outweighed by the reduced surface area. This was observed when comparing PC500, PC105 and PC50 (Table 3). However, the activity ranking of PC10 is puzzling. If the increase in pyridine removal rate in going from PC50 to PC10 was due to the reduced k_r, then a still higher increase in k would be expected for anisole and the phenols, for which the counterbalancing reduction in surface area should not be as important. In fact, the increases in k were low except for anisole, but even for this compound it was lower than for pyridine (Table 3). Analogously, if the increase in pyridine removal rate stemmed from the beneficial effect of traces of rutile [3,15,16] in PC10, similar increases would be expected for anisole and the phenols, unless it is supposed that pyridine removal is especially sensitive to rutile, as has been reported for other photocatalytic reactions [17].

Two of us have suggested [3] that some of the explanation for the high activity toward pyridine of PC10 compared to PC50 may be found in an NMR study which showed that an increased sintering temperature can lead to thinner tightly bound surface water layers [18]. This would facilitate the penetration of solutes through immobile water layers to the catalyst surface, raising photocatalytic rates specifically for those molecules, like pyridine, that react principally by a surface-based mechanism. In particular, for such molecules, this effect serves to offset the reduced surface area caused by high sintering temperatures. It may also improve the access of anisole to the surface, since anisole has a low aqueous solubility (Table 2), which is consistent with weak hydrogen-bonding with water. This effect could therefore explain the higher degradation rate for anisole than for phenol over PC10, despite phenol's higher ring electron density (Table 3).

4-CBA can be decarboxylated by reaction with holes and hydroxylated by reaction with either holes or $^{\bullet}OH$ radicals. As k was found to increase with sintering temperature (Table 3), $^{\bullet}OH$ radical-mediated ring hydroxylation appears to be the main reaction pathway under our conditions. The formation of hydroxybenzoic acids from benzoic acid demonstrates this possibility [19]. The impact of surface-dependent decarboxylation was reflected by a lower overall increase in k than for anisole and the phenols when comparing PC10 to PC500 (Table 3). However, direct comparison of the removal rate of 4-CBA to those of the other aromatic probes should be regarded with caution, as it is complicated by the extent of adsorption, which depends on the TiO_2 sample for 4-CBA and was undetectable for the others.

A key hypothesis in our argumentation to interpret the net effect of TiO_2 sintering temperature is that primary photocatalytic events can occur within the near-surface solution layers. To verify this hypothesis, our approach has been to use

photocatalytic coatings in which the accessibility of reactants to TiO_2 is restricted by the embedding effect of a silica binder, and to determine whether the poor accessibility similarly affects the removal rates of various probe molecules. The answer should allow one to assess the relative importance of close contact between the pollutant and the surface, depending on the probe. As shown in Fig. 4, the restricted accessibility – which was assessed by SEM–EDX (Fig. 2) and oxygen isotope hetero-exchange (Fig. 3) – very differently affected the removal rates of DCAA, 4-CBA and 4-CP. Free access of DCAA to TiO_2 is a prerequisite: the removal is almost totally suppressed for coated TiO_2. TiO_2 accessibility is less important for 4-CBA, and still less for 4-CP. These results are consistent with the hypothesis of hole-mediated decarboxylation occurring on the surface and $^{\bullet}OH$ radical-mediated ring hydroxylation able to take place at some distance from the surface.

This conclusion is further substantiated by comparing the removal of organics in water with $^{18}O_2$–$Ti^{16}O_2$ isotopic exchange, which occurs on the surface. In Fig. 5, the isotopic exchange rates for coated versus powder TiO_2 are plotted against the corresponding aqueous removal rates of 4-CP and 4-CBA, with all values normalized. Results are shown for PC50 and the TiO_2 coatings with two different sizes of SiO_2 binders and an initial $^{18}O_2$ pressure of 11 Pa. These results were virtually identical within the examined range of 2–50 Pa. For 4-CBA, the removal rates were roughly proportional to the isotopic exchange activity, but 4-CP behaved very differently. This supports a mechanism for 4-CBA removal, but not for 4-CP removal, that requires access to the TiO_2 surface. The much greater rate reduction for DCAA removal (Fig. 4) than for isotope exchange can be explained by the high solubility of DCAA (Table 2), which tends to partition to the water phase and therefore has more difficulty than O_2 in accessing the TiO_2 surface. It should be noted, however, that these comparisons must be regarded as semi-quantitative because of the very different experimental conditions.

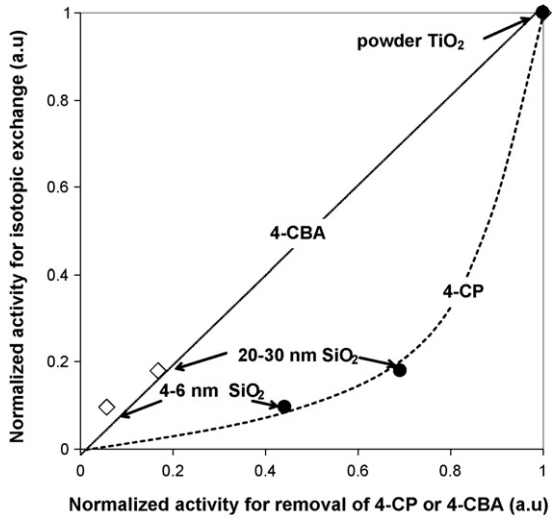

Fig. 5. Comparative plots of the rates of $^{18}O_2$–$Ti^{16}O_2$ isotopic exchange and 4-CBA or 4-CP removal for TiO_2 PC50, either powdered or coated with the SiO_2 indicated.

5. Conclusions

By use of appropriately chosen TiO_2 samples and organic probe molecules, we have shown clear differences among reactants regarding the response of their photocatalytic removal rates in water to different TiO_2 sintering temperatures. Our interpretation of these differences validates intuitive expectations regarding mechanisms that (i) require direct contact between the pollutant and TiO_2 or (ii) can operate over a distance. To wit, direct attack on a pollutant by TiO_2 holes, the mechanism involved in decarboxylation and pyridine ring opening, is much more sensitive to surface area variation than the $^{\bullet}OH$ radical mechanism involved in hydroxylation of the aromatic ring under identical conditions. In addition, when TiO_2 becomes partially inaccessible as a result of the method used to support it, markedly lower decreases in removal rates (Fig. 4) were observed for 4-CP, a molecule reacting predominantly through the $^{\bullet}OH$ radical-mediated mechanism, compared with 4-CBA and DCAA which react, respectively, partially or very predominantly with holes. Likewise, no change in kinetic order was found for 4-CP removal photocatalyzed by affixed TiO_2 with respect to powder TiO_2, whereas a decrease from 1 to 0 was found for 4-CBA. These observations are all consistent with the possibility for the $^{\bullet}OH$ radical to react at some distance from the surface.

Acknowledgements

The authors warmly thank Mr. B. Beaugiraud, H. Courbon, J. Disdier and Mrs. M.-N. Mozzanega (CNRS) for their advice about the experiments. R.E. is grateful to the CONACYT (Mexico) for financial support. The gift of samples by Millennium Chemicals, Ahlstrom and Rhodia is gratefully acknowledged.

References

[1] A. Fujishima, K. Hashimoto, T. Watanabe, TiO_2 Photocatalysis, BKC, Tokyo, 1999.
[2] P. Pichat, in: M.A. Tarr (Ed.), Chemical Degradation Methods for Wastes and Pollutants: Environmental and Industrial Applications, Marcel Dekker Inc., New York, Basel, 2003, p. p77.
[3] A.G. Agrios, P. Pichat, J. Photochem. Photobiol. A 180 (2006) 130.
[4] R. Enriquez, PhD Dissertation, École Centrale de Lyon, Ecully, France, 2002.
[5] R. Enriquez, B. Beaugiraud, P. Pichat, Water Sci. Technol. 49 (2004) 147.
[6] J.M. Warman, M.P. de Haas, P. Pichat, T.P.M. Koster, E.A. van der Zouwen-Assing, A. Mackor, R. Cooper, Radiat. Phys. Chem. 37 (1991) 433.
[7] E. Mietton-Ceulemans, PhD Dissertation, Université Lyon 1, France, 2001.
[8] Ahlstrom, French patent no. PCT/FR 99/00748 (1999).
[9] J. Cunningham, G. Al-Sayyed, S. Srijaranai, in: G.R. Helz, R.G. Zepp, D.G. Crosby (Eds.), Aquatic and Surface Photochemistry, Lewis, Boca Raton, FL, 1994, p. 317.
[10] M.W. Peterson, J.A. Turner, A.J. Nozik, J. Phys. Chem. 95 (1991) 221.
[11] C.S. Turchi, D.F. Ollis, J. Catal. 122 (1990) 178.
[12] B. Kraeutler, A.J. Bard, J. Am. Chem. Soc. 99 (1977) 7729.
[13] L. Cermenati, P. Pichat, C. Guillard, A. Albini, J. Phys. Chem. B 101 (1997) 2650.

[14] L. Cermenati, A. Albini, P. Pichat, C. Guillard, Res. Chem. Intermed. 26 (2000) 221.
[15] A.G. Agrios, K.A. Gray, E. Weitz, Langmuir 19 (2003) 1402.
[16] D.C. Hurum, A.G. Agrios, K.A. Gray, T. Rajh, M.C. Thurnauer, J. Phys. Chem. B 107 (2003) 4545.
[17] H. Kominami, S. Murakami, J.-I. Kato, Y. Kera, B. Ohtani, J. Phys. Chem. B 106 (2002) 10501.
[18] A.Y. Nosaka, T. Fujiwara, H. Yagi, H. Akutsu, Y. Nosaka, J. Phys. Chem. B 108 (2004) 9121.
[19] R.W. Matthews, J. Chem. Soc. Faraday Trans. 80 (1984) 457.